Eur. Phys. J. B **55**, 77–84 (2007)
DOI: 10.1140/epjb/e2007-00042-6

THE EUROPEAN PHYSICAL JOURNAL B

Magnetic structures and crystal field in the heavy electron materials YbAgGe and YbPtIn

P. Bonville[1,a], M. Rams[2], K. Królas[2], J.-P. Sanchez[3], P.C. Canfield[4], O. Trovarelli[5], and C. Geibel[5]

[1] Commissariat à l'Énergie Atomique, Centre de Saclay, DSM/SPEC, 91191 Gif-sur-Yvette Cedex, France
[2] Institute of Physics, Jagiellonian University, 30-059 Kraków, Poland
[3] Commissariat à l'Énergie Atomique, Centre de Grenoble, DSM/SPSMS, 38054 Grenoble, France
[4] Ames Laboratory, Iowa State University, Ames IA 50011, USA
[5] Max Planck Institute for Chemical Physics of Solids, 01187 Dresden, Germany

Received 24 October 2006 / Received in final form 26 January 2007
Published online 9 February 2007 –

Abstract. We have examined the magnetic properties of the heavy electron compounds YbAgGe and YbPtIn by ^{170}Yb Mössbauer spectroscopy down to 0.1 K, and the crystal field properties of YbAgGe by Perturbed Angular Correlations (PAC) measurements up to 900 K. In YbAgGe, we show that each of the two magnetically ordered phases below 0.8 K involves a specific incommensurate modulation of the Yb moment. An analysis of existing low temperature specific heat data suggests the persistence of fluctuations of the correlated Yb spins down to 0.1 K. The PAC data allow to discriminate among proposed Yb^{3+} crystal field level schemes. In YbPtIn, we show that the low temperature magnetic order phase has an antiferro-para structure, where zero moment Yb ions coexist with large moment ones, and that a 90° moment reorientation occurs at 1.4 K.

PACS. 71.27.+a Strongly correlated electron systems; heavy fermions – 76.80.+y Mossbauer effect; other gamma-ray spectroscopy

1 Introduction

Some ternary Yb intermetallics crystallizing in the hexagonal ZrNiAl-type structure combine two features which are hot topics in present solid state magnetism: the Kondo effect and geometrical frustration of the magnetic interactions. The Kondo effect, due to a hybridisation between $4f$ and conduction electrons, leads to a shielding of the local $4f$ moment at low temperature resulting in a non-magnetic singlet N-electron ground state and to the formation of the so-called heavy electrons [1]. Geometrical frustration of interionic magnetic interactions occurs in special lattice types, like triangular, *kagomé* or pyrochlore [2], where the vertices are occupied by a magnetic species. Frustration can prevent long range ordering (LRO) of the magnetic moments down to $T = 0$, for instance in the case of an antiferromagnetic (AF) Heisenberg system. However, the long range nature of the RKKY exchange interaction in Kondo lattices, and the presence of magnetic anisotropy, of dipole-dipole and other higher order interactions in frustrated lattices, generally stabilize a LRO ground state. Then the magnetic structures, resulting of an equilibrium between antagonist interactions, can show very unusual or exotic features.

In the two compounds YbAgGe and YbPtIn, which have a ZrNiAl-type structure, the Yb magnetic ions are located on the vertices of coplanar corner-sharing triangles (see Fig. 1), i.e. they are arranged in a *kagomé*-like lattice, prone to frustration of AF interactions. Measurements of thermodynamic and transport properties have been carried out in YbPtIn [3,4] and YbAgGe [5,6], showing somewhat analogous features: the crystal **c** axis is a hard magnetic axis, the paramagnetic Curie temperature θ_p is negative with a magnitude of a few 10 K, indicative of AF exchange and/or Kondo coupling, and two magnetic transitions are observed below 4 K. In YbPtIn, they occur at 1.4 and 3.4 K [4], and in YbAgGe at 0.65 and 0.8 K according to reference [7], and at 0.65 K and 1 K according to reference [8]. Heavy electron behaviour is also reported for both compounds as a high value of the Sommerfeld coefficient $\gamma = \lim_{T\to 0} C_{el}(T)/T$, where C_{el} is the electronic specific heat. It was found that $\gamma \simeq 500\ \mathrm{mJ/mol\,K^2}$ for YbPtIn [4] and that it lies in the range 150 to 1000 $\mathrm{mJ/mol\,K^2}$ in YbAgGe [5,6,9]. The $H - T$ phase diagram around the field induced quantum critical point was extensively studied by transport measurements down to very low temperature in YbAgGe [8–10] and in YbPtIn [11]. Finally, the low temperature magnetic and anisotropy properties have been investigated in both the RAgGe series [6] and the RPtIn series [12], where R = Gd-Tm.

[a] e-mail: bonville@dsm-mail.saclay.cea.fr

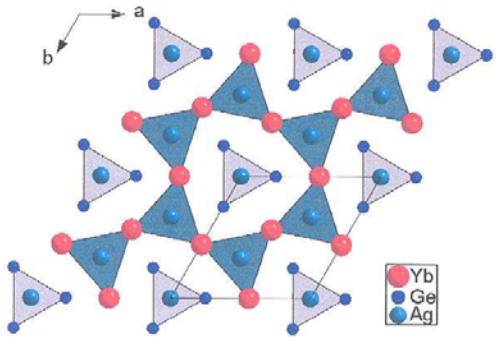

Fig. 1. (Color on line) Projection of the YbAgGe crystal structure onto the base (**a**, **b**) plane: Yb in the $3g$ sites (x, 0, 1/2), (0, x, 1/2) and ($\bar{x}, \bar{x}, 1/2$) in the $z = 1/2$ plane, and Ge in the $3f$ sites (x, 0, 0), (0, x, 0) and ($\bar{x}, \bar{x}, 0$) in the $z = 0$ plane.

Some hints about the crystal field levels have been obtained by inelastic neutron scattering in YbAgGe: a single excitation was found at 12 meV [13]. The magnetic structure in YbAgGe has been investigated by neutron diffraction [14,15], but the determination of the number and nature of the magnetic phases is still underway. The magnetic Bragg peaks observed below 0.65 K could be indexed with a propagation vector $\mathbf{k} = (1/3, 0, 1/3)$, and those in the phase 0.65 K $< T <$ 0.8 K with the incommensurate vector $\mathbf{k} = (0, 0, 0.324)$. Recent neutron diffraction data [16] suggest that there are in fact three magnetic transitions in YbAgGe, at 0.65, 0.8 and 1 K. In the following, we will adopt this result, keeping in mind that the exact nature of the phase 0.8 K $< T <$ 1 K is not yet established.

In this work, we report on a ^{170}Yb Mössbauer spectroscopy investigation of YbAgGe and YbPtIn, in zero magnetic field, down to 0.1 K, together with ^{172}Yb Perturbed Angular Correlations (PAC) measurements in YbAgGe up to 900 K. Through these local techniques, we could gain new insight in the magnetic moment magnitude and orientation in the LRO phases of both compounds: we find that YbAgGe presents modulated magnetic structures, and that YbPtIn has the so-called antiferro-para structure as ground state. In YbAgGe, our PAC data allow to discriminate between proposed crystal field models. Using the hyperfine parameters derived from the Mössbauer data in YbAgGe, we also interpret the very low temperature specific heat measurements of reference [9] and show that collective spin fluctuations are present in the magnetic LRO phase.

2 Experimental

The experiments were performed on a powder YbAgGe sample obtained by grinding single crystals, and on a polycrystalline YbPtIn sample. The preparation details are given in reference [4] for YbPtIn and in reference [6] for YbAgGe. Both compounds crystallize in the $P\bar{6}2m$ space group, with 3 equivalent Yb sites in the unit cell, and the point symmetry at the Yb site is C_{2v}. For Yb at $(x, 0, 1/2)$, the two mirror planes are (**a**, **b**) and (**a**, **c**) planes, and **a** (or [100]) is the two-fold symmetry axis. For the other Yb sites at $(0, x, 1/2)$ and $(\bar{x}, \bar{x}, 1/2)$, the two-fold axis is respectively [010] and [110]. The lattice parameters of the hexagonal unit cell are: $a = 7.548$ Å and $c = 3.766$ Å for YbPtIn, and $a = 7.05$ Å and $c = 4.14$ Å for YbAgGe.

The ^{170}Yb Mössbauer measurements ($E_0 = 84.3$ keV, $I_g = 0$, $I_e = 2$) were performed with a Tm^*B_{12} γ-ray source mounted on an electromagnetic drive with triangular velocity signal (1 mm/s = 68 MHz). For the PAC measurements, the sample was proton irradiated to produce ^{172}Lu nuclei and annealed at 800 °C to remove irradiation defects. We used the 91–1094 keV $\gamma-\gamma$ cascade from the $^{172}\text{Lu} \mapsto {}^{172}\text{Yb}$ β decay; the intermediate level of the cascade, namely the 1172 keV excited state of ^{172}Yb has a spin $I = 3$. More details about ^{172}Yb PAC measurements are given in reference [17].

3 YbAgGe: crystal electric field and magnetic structures

3.1 The 4f quadrupole moment and the crystal field

Combined Mössbauer and PAC measurements [17] yield very useful information for determining the crystal electric field (CEF) level scheme in Yb compounds. The $J = 7/2$ ground spin-orbit multiplet of the Yb^{3+} ion is split by the CEF interaction into 4 Kramers doublets. Each doublet has a well-defined $4f$ quadrupolar tensor:

$$Q^{4f}_{i,j} = \left\langle \frac{3}{2}(J_i J_j + J_j J_i) - J(J+1)\ \delta_{i,j} \right\rangle, \qquad (1)$$

which gives the main contribution to the hyperfine interaction with the nuclear quadrupole moment. Another contribution, usually smaller, stems from the lattice (ionic charges on all neighboring atoms and contribution from the conduction electrons). The total hyperfine quadrupolar interaction writes:

$$\mathcal{H}_Q = \alpha_Q \left[I_Z^2 - \frac{I(I+1)}{3} + \frac{\eta}{6}(I_+^2 + I_-^2) \right], \qquad (2)$$

where the parameters α_Q and η (asymmetry parameter) are expressed in terms of the main components (V_{XX}, V_{YY}, V_{ZZ}) of the electric field gradient tensor (EFG) at the Yb nucleus site:

$$\alpha_Q = \frac{3eQV_{ZZ}}{4I(2I-1)} \quad \text{and} \quad \eta = \frac{|V_{YY} - V_{XX}|}{|V_{ZZ}|}, \qquad (3)$$

Q being the nuclear quadrupole moment. The axis OZ is the principal axis of the EFG tensor, i.e. $|V_{ZZ}|$ corresponds to the largest eigenvalue. As the Yb site symmetry is C_{2v}, the main axes of the EFG tensor for Yb at $(x, 0, 1/2)$ are **a**, **c** and a third axis perpendicular to **a** and **c**, and the corresponding axes rotated by 120° and 240° around **c** for the two other sites. For non-axial point symmetry, it is not known a priori which is the principal axis.

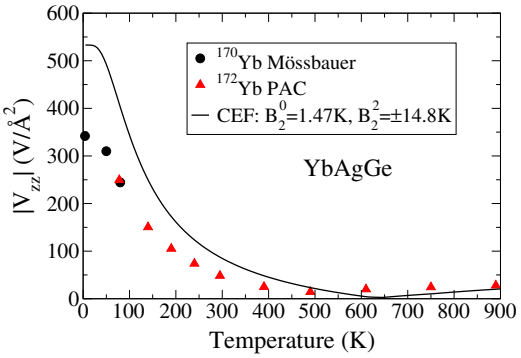

Fig. 2. (Color on line) Thermal variation of the absolute value of the principal component V_{ZZ} of the electric field gradient at the Yb site, as measured by ^{170}Yb Mössbauer spectroscopy (circles) and ^{172}Yb PAC (triangles) measurements between 4.2 K and 900 K. The solid line is calculated from a crystal field model (see text).

The $4f$ shell contribution to the EFG tensor is proportional to the thermal average of the $4f$ quadrupole tensor. It shows a strong thermal variation, for trivalent Yb ions, because it depends on the equilibrium populations of the CEF levels. For instance, its principal value writes:

$$V_{ZZ}^{4f}(T) = B_Q \langle 3J_Z^2 - J(J+1) \rangle_T, \qquad (4)$$

where $B_Q \simeq 29$ V/Å^2 for Yb^{3+}.

The quantities V_{ZZ} and η were measured in the paramagnetic phase, using ^{170}Yb Mössbauer spectroscopy between 4.2 and 80 K (see next section), and using ^{172}Yb PAC (which gives access only to $|V_{ZZ}|$) between 80 and 900 K. The η value is found to be close to 0.1–0.2 below 400 K. At 4.2 K, the ^{170}Yb quadrupolar coupling parameter is $\alpha_Q \simeq 3.2(1)$ mm/s, which corresponds to $V_{ZZ} \simeq -340$ V/Å^2. As temperature increases, V_{ZZ} presents a significant thermal variation, typical for a Yb ion with a valence close to 3, and shown in Figure 2. The quantity $V_{ZZ}(T)$ can be calculated from the eigenvalues and eigenfunctions of the crystal field Hamiltonian: $\mathcal{H}_{CEF} = \sum_{n,m} B_n^m O_n^m$, where the O_n^m are Stevens crystal field operator-equivalents [19]. For the C_{2v} point symmetry of the Yb site, all B_n^m parameters with even n and m enter the expression of $\mathcal{H}_{CEF}$.

A simplified model CEF interaction for YbAgGe, using only the two lowest order parameters ($B_2^0 = 1.47$ K and $B_2^2 = \pm 14.8$ K) has been put forward in reference [13]; it yields a ground state with magnetic hard axis along **c** and a first excited state at an energy 12 meV above the ground state, as experimentally observed. The solid line in Figure 2 is calculated using these model parameters, and an estimated small lattice gradient: $|V_{ZZ}^{latt}| = 70$ V/Å^2. The agreement with experiment is qualitatively good, although the calculated curve lies above the data points. However, it is known that the Kondo coupling can strongly reduce the CEF only calculated V_{ZZ} values [18], by mixing the single ion wave-functions with extended conduction states. In YbAgGe, the Kondo coupling is thought to be rather large ($T_K \sim 25$ K), so that it was not attempted nor to refine the two B_n^m parameters, neither to use a greater number of parameters, in order to obtain a better match to the experimental V_{ZZ} data. This crude CEF model yields however a much better agreement with experiment than that proposed in reference [5] ($B_2^0 = 0.085$ K, $B_4^0 = 0.061$ K and $B_4^2 = -1.0$ K), which yields $|V_{ZZ}|$ values below 20 V/Å^2 in the whole temperature range.

Using the parameter values $B_2^0 = 1.47$ K and $B_2^2 = -14.8$ K, and choosing the two-fold axis (i.e. [100], [010] or [110] respectively for the 3 Yb sites in the unit cell) as the quantisation z-axis, the wave function of the ground doublet is very close to: $|\psi_0\rangle = |J = 7/2;\ J_z = \pm 7/2\rangle$. This corresponds to a very anisotropic g-tensor: $g_c \simeq 0$ and $g_a \simeq 8$ [19,20]. This two-fold axis is also the principal axis OZ of the electric field gradient tensor. Taking into account the crudeness of the model CEF interaction used here, it is likely that the actual g-tensor of the Yb^{3+} ground doublet does not present such an extreme anisotropy.

3.2 The ^{170}Yb Mössbauer absorption spectra

^{170}Yb Mössbauer spectra in YbAgGe at selected temperatures are shown in Figure 3. At 4.2 K and up to 80 K, the spectrum is a quadrupolar hyperfine spectrum typical for the paramagnetic phase, and the line positions can be fitted to the eigenvalues of Hamiltonian (2), yielding the α_Q and η values as described in the previous paragraph.

Below 1 K, the spectra at 0.1 K, 0.6 K (not shown) and 0.73 K present a resolved magnetic hyperfine structure. In a LRO phase, the ^{170}Yb Mössbauer spectra show 5 absorption lines with equal intensities arising from the Zeeman splitting of the excited nuclear state with spin $I_e = 2$. The lineshapes observed in YbAgGe below 0.75 K are peculiar, i.e. they present strong inhomogeneous line broadenings and the 5 lines are not individually resolved. These spectral shapes can be due to a continuous distribution of the magnitude and/or of the orientation of the hyperfine field. However, they do not correspond to a standard Gaussian shaped distribution. They rather remind of the spectrum of a modulated magnetic structure, either with an incommensurate wave-vector, as observed in YbPtAl [21], or with a commensurate, but very small wave-vector. This latter assumption can however be discarded since the neutron diffraction spectra could be indexed with propagation vectors of magnitude of order unity. For ^{170}Yb, the spectral signature of an incommensurate modulation is the presence of a very broad and "flat" line at the right edge of the spectrum. For non S-state rare earths, the hyperfine field is proportional to the magnetic moment, with a proportionality constant $C = 102$ T/μ_B for Yb^{3+}.

As a first assumption, we analysed the spectra in the M1 phase ($T < 0.65$ K) and M2 phase (0.65 K $< T <$ 0.8 K) in terms of an amplitude modulation, the orientation of the moment in the main axes of the EFG tensor being kept fixed. The moment modulation is described by a sine-Fourier expansion up to the fifth harmonics. For a given position x of a Yb ion along the propagation

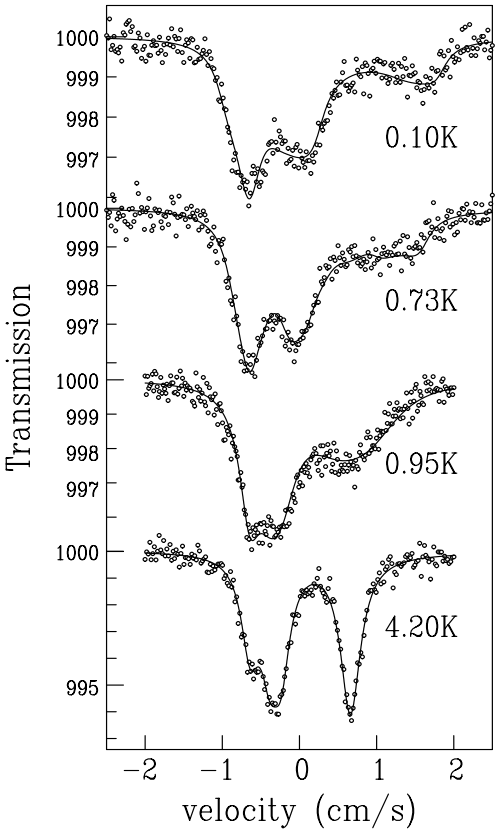

Fig. 3. ^{170}Yb Mössbauer absorption spectra in YbAgGe in the four phases: M1 ($T < 0.65$ K), M2 (0.65 K $< T <$ 0.8 K), M3 (0.8 K $< T <$ 1 K) and P (paramagnetic, $T > 1$ K). The lines are fits to an incommensurate modulation of the Yb moments at 0.1 and 0.73 K, to a longitudinal spin fluctuation lineshape at 0.95 K, and to a pure quadrupole hyperfine interaction at 4.2 K.

vector **k**, the moment value is thus:

$$m(kx) = m_1 \sin kx + m_3 \sin 3kx + m_5 \sin 5kx. \quad (5)$$

To each moment value along the **k** direction corresponds a hyperfine field $H_{hf}(kx) = Cm(kx)$, and the associated spectrum is obtained from the hyperfine Hamiltonian:

$$\mathcal{H}_{hf} = -g_n\mu_n \mathbf{H_{hf}}.\mathbf{I} + \mathcal{H}_\mathbf{Q}, \quad (6)$$

where $g_n\mu_n\mathbf{I}$ is the nuclear magnetic moment and $\mathcal{H}_Q$ is the quadrupolar Hamiltonian (2). The final spectrum is computed by summing the individual spectra over the kx values between 0 and 2π with a constant density, the adjustable parameters being the Fourier components m_1, m_3 and m_5 and the angle θ between the principal axis OZ of the EFG tensor and the moment direction. A good fit of the 0.1 K spectrum is obtained with the parameters:

$$m_1 = 1.435\,\mu_B; \quad m_3 = 0.017\,\mu_B; \quad m_5 = 0.049\,\mu_B. \quad (7)$$

This corresponds to the modulation shown in Figure 4 and to the peculiar moment distribution shown in the inset of Figure 4. The maximum moment value is $\simeq$1.5 μ_B, and

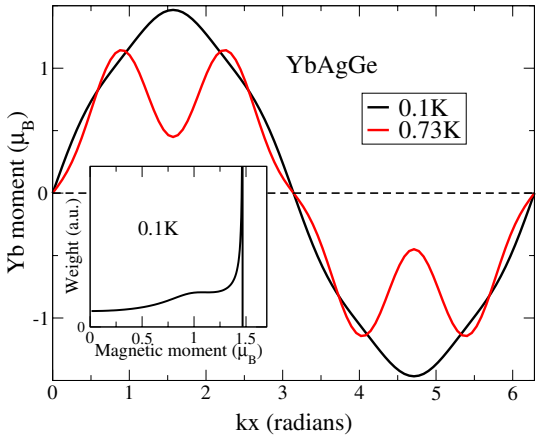

Fig. 4. (Color online) Yb moment modulation in YbAgGe, at 0.10 K (M1 phase) and 0.73 K (M2 phase), derived from the ^{170}Yb Mössbauer spectra. Inset: distribution of moment amplitudes at 0.1 K.

the modulation is almost a pure sine-wave. This maximum moment value is much lower than that inferred from the approximate CEF model described in section 3.1 ($m_0 = \frac{1}{2}g_a\mu_B \simeq 4\ \mu_B$). This can be partly ascribed to the Kondo screening of the magnetic moment.

At 0.6 K, the modulation is identical to that at 0.1 K, which suggests that the transition from phase M1 to M2 is sharp and possibly first order, as noted previously [7]. At both temperatures, we obtain a good fit with a unique angle $\theta \leq 10°$.

The spectrum shape changes slightly, but significantly, at 0.73 K, in the M2 magnetic phase. A good fit is obtained with the Fourier components:

$$m_1 = 1.00\,\mu_B; \quad m_3 = 0.32\,\mu_B; \quad m_5 = -0.23\,\mu_B, \quad (8)$$

and the same θ angle of at most 10°. The corresponding modulation is shown in Figure 4. The maximum moment value is about 1.2 μ_B, and the modulation is different from that in the M1 phase.

As a second assumption, a helicoidal magnetic structure with constant moment value and incommensurate pitch was tried. The spectra at 0.1 and 0.73 K can be reproduced with this hypothesis, the Yb moments having the values respectively 1.55 and 1.35 μ_B and being close to perpendicular to the propagation vector. The fits are not of as good quality as with the amplitude modulation fit, but this second assumption cannot be completely discarded.

In the M3 phase at 0.85 K (spectrum not shown) and 0.95 K, the magnetic hyperfine pattern is smeared out and the spectra are characteristic of a fluctuating hyperfine field, i.e. they belong to a phase with dynamic spin correlations. The best relaxation model to fit these spectra is a longitudinal model where the hyperfine field fluctuates along the Z axis. The fit yields a Yb moment of about 1 μ_B fluctuating with a frequency $\nu \simeq 2.6 \times 10^9$ s^{-1} at 0.85 K and 3.6×10^9 s^{-1} at 0.95 K. Phase M3 could be a paramagnetic phase with short range correlations or a LRO phase with rapidly fluctuating Yb moments.

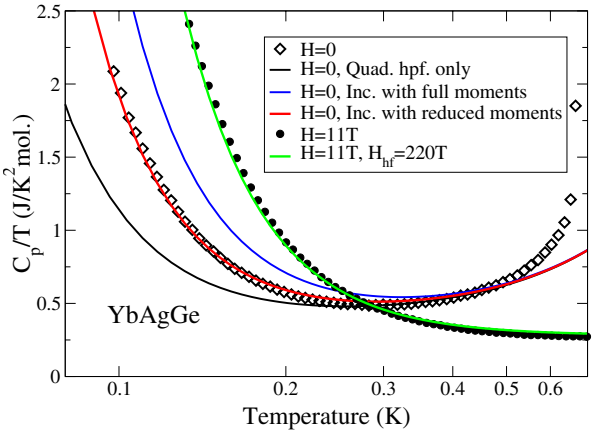

Fig. 5. (Color online) Semi-log plot of the low temperature specific heat in YbAgGe in zero field (open symbol) and with a field of 11 T applied in the (**a, b**) plane (closed circle) from reference [9]. The lines are calculated using various assumptions about the hyperfine parameters (see text).

At 4.2 K, the fast relaxation regime is reached ($\nu > 10^{10}$ s^{-1}) and the magnetic pattern has disappeared, leaving a quadrupolar hyperfine spectrum.

3.3 The very low temperature specific heat

The specific heat of a single crystal of YbAgGe has been measured down to the 0.1 K range, in zero field and with fields up to 11 T applied in the basal (**a, b**) plane [9]. It was shown that the magnetic transition is cancelled for fields above 5 T. The data curves show a Schottky hyperfine upturn below 0.2 K (Fig. 5), which arises from the quadrupolar and magnetic hyperfine splittings of the ground nuclear level of the isotopes ^{171}Yb ($I_g = 1/2$) and ^{173}Yb ($I_g = 5/2$) in the M1 phase. Note that the quadrupolar contribution comes solely from the ^{173}Yb isotope, which has a quite large quadrupolar moment in its ground nuclear state: $Q^{173} = 3.1$ b. The hyperfine Schottky anomalies can be computed from Hamiltonian (6) using the electronic dipole and quadrupole moments derived from the Mössbauer spectra in phase M1, and compared with experiment. The calculated curves in Figure 5 are the sum of the Schottky hyperfine specific heat and of two electronic contributions:

$$C_p = C_{Schottky} + \gamma T + bT^3, \qquad (9)$$

where γ is the electronic Sommerfeld coefficient and b the spin-wave coefficient.

For the $H = 0$ data, $\gamma = 0.37$ J/K^2 mol. and $b = 1$ J/K^4 mol. reproduce correctly the electronic part in the range 0.2–0.5 K, in good agreement with reference [9] as concerns the $\gamma(H = 0)$ value. The calculated nuclear Schottky term, derived from the measured quadrupolar interaction and magnetic hyperfine splittings due to the moment distribution in the M1 phase (inset of Fig. 4) is shown as the blue line in Figure 5. Unexpectedly, it lies above the experimental points. If one considers the quadrupolar interaction alone, the corresponding curve (black line in Fig. 5) lies below the experimental data. This can be interpreted as a reduction of the magnetic contribution to the hyperfine Schottky anomaly due to fluctuations of the correlated Yb spins [22]. This reduction effect occurs in the magnetic LRO phase in case the spin fluctuation time τ and the nuclear (hyperfine) relaxation time T_1 are of the same magnitude. The physics underlying this phenomenon is that, in case $T_1 \sim \tau$, the hyperfine levels have no time to thermalise before the moment (i.e. the hyperfine field) switches again. Then the steady state out of equilibrium hyperfine populations are reduced, leading to a scaled decrease of the Schottky specific heat.

It was shown in reference [22] that, for a model spin 1/2, the hyperfine Schottky specific heat is reduced by a factor $r = 1 + 2T_1/\tau$, and the effective moment derived from this Schottky anomaly is reduced by $\sqrt{r}$. In order to obtain the r factor in YbAgGe, the experimental data was fitted to the quadrupolar interaction and magnetic incommensurate structure, but allowing for a common reduction of all the moment values. The red line in Figure 5 reproduces the zero field data, with $\sqrt{r} = 1.54$. This corresponds to a ratio of the hyperfine relaxation time to the fluctuation time of the correlated Yb moments $T_1/\tau \sim 0.68$, keeping in mind that this evaluation is only strictly exact for a nuclear spin 1/2. Very few measurements are available of the relaxation time T_1 at such low temperature; hyperfine relaxation is probably due to coupling to spin-waves, and one can speculate that T_1 lies in the range 10^{-4}–10^{-7} s. As to τ, the observation of fully developed static hyperfine field Mössbauer spectra indicates that it is longer than 10^{-8} s. Therefore, the analysis of the specific heat data in the light of the ^{170}Yb Mössbauer data strongly suggests the presence of fluctuations of the correlated Yb moments in the LRO M1 phase of YbAgGe. Spin fluctuations have been evidenced by this method in the LRO phase of the frustrated "ordered spin ice" pyrochlore $Tb_2Sn_2O_7$ [23].

For the $H = 11$ T specific heat curve, there is no magnetic transition and accordingly the spin-wave coefficient b is found to be zero; the Sommerfeld coefficient $\gamma(11$ T) is reduced to 0.28 J/K^2 mol., and a good fit to the data is obtained by assuming a single hyperfine field of 220 T (green line in Fig. 5). Neglecting the applied field, this corresponds to a mean Yb polarisation of *ca.* 2.2 μ_B. As the spin fluctuations are likely to be frozen by the high magnetic field, this should represent the actual value of the static Yb^{3+} moment under field. This value is larger than the zero field moment values (maximum 1.5 μ_B), which can have two explanations: the magnetic field depletes the Kondo coupling, resulting in a weaker screening of the magnetic moment, and/or the CEF mixing due to the magnetic field enhances the ground state Yb moment. The 11 T moment value derived from the specific heat is also larger than the magnetisation in the (**a, b**) plane measured with the same field at 0.05 K (1.4 μ_B) [9]. The Schottky anomaly, through the hyperfine field, measures the magnitude of the magnetic moment, and the smaller

value of the magnetisation, i.e. of the projection of the moment on the field direction, can be due to an incomplete alignment of the moments along the field. This is also witnessed by the absence of saturation of the magnetisation at 11 T.

3.4 Discussion

According to the neutron diffraction data on a single crystal sample [14], the propagation vector of the magnetic structure in phase M1 is $\mathbf{k} = (1/3, 0, 1/3)$, i.e. it is commensurate with the lattice spacings, whereas the Mössbauer data point towards an incommensurate modulation. The diffraction pattern shown in reference [14] indeed presents a sixfold symmetry, but no uncertainty on the wave-vector components is quoted. An small incommensurability of one of the components of the **k** vector (or of both components) would be reflected in a finite size of the diffraction spots, and could remain undetected in the neutron data analysis. In phase M2, the incommensurability of the propagation vector obtained from the neutron diffraction data [15] is in agreement with the Mössbauer results.

So, contrary to what had been speculated previously [6], YbAgGe is not a small moment ordered system, but shows a moment modulation with a sizeable maximum value (1.5 μ_B in the M1 phase, 1.2 μ_B in the M2 phase). The assumption of a small ordered Yb moment in YbAgGe had been put forward because of the very small value of the entropy release at 1 K, i.e. at the transition from the M3 magnetic phase to the paramagnetic phase ($\sim$10% of $R \ln 2$ [6,7]). Actually, this reduction can arise from three phenomena in YbAgGe: i) the Kondo coupling, because the paramagnetic degrees of freedom are not entirely released at the magnetic transition [1]; ii) the incommensurability of the magnetic structure, because the presence of moment values between zero and the maximum value of the modulation reduces the specific heat jump at the transition, and hence the entropy, by a factor 2/3 [24]; iii) and possibly the frustration of the exchange interaction on the *kagomé*-like Yb lattice [2]. Up to now, frustration in these materials has not been demonstrated to exist. The study of thermodynamic and transport properties in the RAgGe series, where R = Tb-Lu [6], has shown that the easy magnetic axis is the **c** axis, except for the Er, Tm and Yb members of the series which have strong planar (**a, b**) anisotropy. Frustration can arise on a *kagomé* lattice with Ising moments perpendicular to the plane and antiferromagnetically coupled. It can be seen that it is also fully operative with in-plane moments either with isotropic ions coupled via antiferromagnetic exchange or with ferromagnetically coupled Ising ions. Exchange is antiferromagnetic in the RAgGe series, and thus the Tm moments in TmAgGe, for instance, which are strongly Ising in the (**a, b**) plane, are not expected to be frustrated. As to YbAgGe, frustration could be present provided the ground doublet has a finite in-plane anisotropy, i.e. if both the g_a and g_b values are sizeable. As concerns frustration, this situation is indeed similar to the isotropic antiferromagnet case. As noted in section 3.1, the Ising-like Yb^{3+} ground wave-function obtained using the model CEF parameters is likely to be a crude approximation. The actual ground g-tensor could show finite planar anisotropy, allowing frustration to play a role in the magnetic properties. This would yield a third source for reduction of the entropy release at T_N and could be the cause of the presence of fluctuations in the LRO phase.

4 YbPtIn: the ^{170}Yb Mössbauer absorption spectra

The ^{170}Yb Mössbauer spectra in the three phases of YbPtIn are represented in Figure 6. At 4.2 K, the paramagnetic quadrupolar hyperfine spectrum yields $\eta \simeq 0.1$ and $\alpha_Q \simeq 4.4$ mm/s (corresponding to $V_{ZZ} \simeq -466$ V/Å^2).

At the lowest temperature (0.08 K) in the M1 phase ($T < 1.4$ K), the spectrum shows a good resolution, but more than 5 lines can be sorted out: this means that two hyperfine contributions are present. The fit shows that this spectrum is well accounted for by the sum of two components: a quadrupolar spectrum with relative intensity 35(2)%, similar to that at 4.2 K but with somewhat broader lines (red line in Fig. 6 top), and a magnetic hyperfine spectrum with relative intensity 65(2)%, with a hyperfine field $H_{hf} \simeq 220$ T parallel to the local quantisation axis OZ ($\theta = 0$). In this latter spectrum, the most energetic line is broader, but well resolved. This is a known effect of the random small crystal field distortions present in the sample [25]. This spectrum corresponds to a large spontaneous Yb^{3+} moment of 2.2 μ_B directed along the principal axis of the EFG tensor, i.e. probably along **a** in the easy magnetic plane. The quadrupolar spectrum corresponds to a Yb^{3+} ion with zero moment (or with a magnetic moment fluctuating faster than 10^{10} s^{-1}). This demonstrates the coexistence, in the M1 phase of YbPtIn, of Yb ions with a large moment (2.2 μ_B at 0.08 K) and of Yb ions with zero moment, in the proportion 2:1. The simplest interpretation is that the M1 phase is an antiferro-para (AFP) commensurate phase, where the moments show an arrangement of the type $\uparrow\downarrow 0 \uparrow\downarrow 0 \ldots$ along the propagation vector **k**. Such structures have been observed in CeSb, but only at finite temperature [26]. As temperature increases, the hyperfine field of the main magnetic component decreases, reaching 120 T at 1.4 K.

As one enters the M2 phase (see spectrum at 1.45 K in Fig. 6), the spectrum abruptly changes: the hyperfine field value drops to about 30 T (i.e. the Yb moment drops to about 0.3 μ_B), and the angle θ between the hyperfine field and the principal axis OZ of the EFG jumps to 90°. The thermal variation of the spontaneous moment in both phases is represented in Figure 7. The transition at 1.4 K corresponds thus to a first order reorientation of the Yb moments towards the hard magnetic **c** axis, which explains the low moment value in the M2 phase.

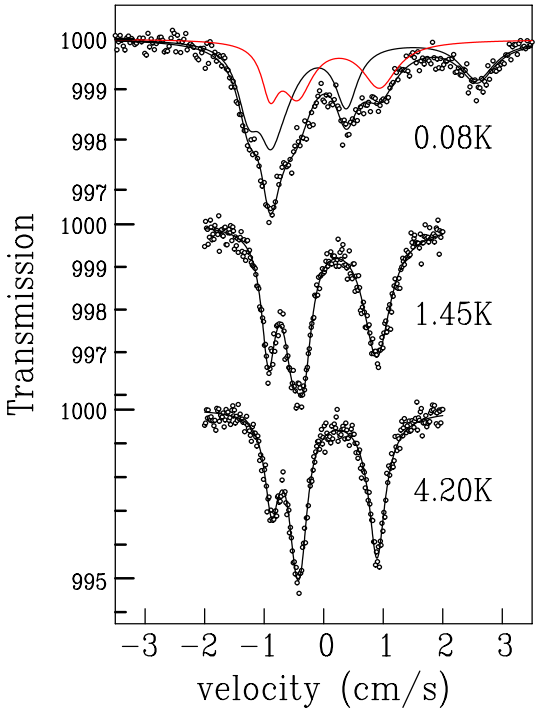

Fig. 6. (Color on line) ^{170}Yb Mössbauer absorption spectra in YbPtIn in the three phases: M1 ($T < 1.4$ K), M2 (1.4 K $< T <$ 3.4 K) and P (paramagnetic, $T > 3.4$ K). The lines are fits to quadrupolar and magnetic hyperfine interactions as explained in the text. At 0.08 K, the subspectrum in red corresponds to zero moment Yb ions.

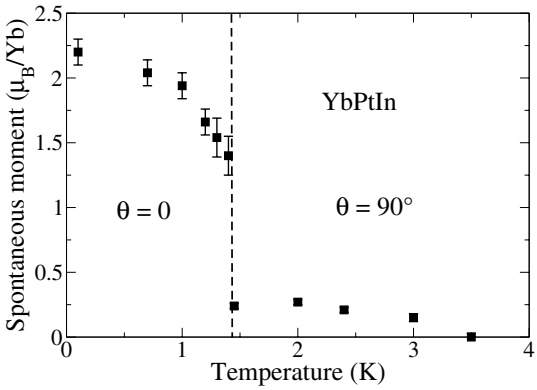

Fig. 7. Thermal variation of the spontaneous Yb moment in YbPtIn as derived from the ^{170}Yb hyperfine field values; the reorientation of the moment near 1.4 K is indicated by the value of the angle θ it makes with the easy magnetic axis in the (**a**, **b**) plane.

5 Summary and conclusion

^{170}Yb Mössbauer and ^{172}Yb Perturbed Angular Correlations spectroscopies applied to the heavy electron materials YbAgGe and YbPtIn in a large temperature range yield valuable information about their low temperature magnetic phases and about the crystal field splittings (in YbAgGe).

In YbAgGe, we showed that each of the two low temperature magnetic phases below 0.8 K has an incommensurate modulated structure with sizeable maximum moment per Yb ion (1.5 μ_B for the ground M1 phase, and 1.2 μ_B for the M2 phase). We showed that the description of the Yb^{3+} crystal field interaction with the two parameters $B_2^0 = 1.47$ K and $B_2^2 = \pm 14.8$ K proposed in reference [13] is a correct first order approximation. Our analysis of the very low temperature Schottky upturn of the specific heat in YbAgGe strongly suggests that the Yb moments keep fluctuating in the magnetically ordered M1 phase. In YbPtIn, we showed that the ground magnetic phase has an antiferro-para structure, where zero moment Yb ions alternate with large moment ions (2.2 μ_B) in the (**a, b**) plane. At 1.4 K, a moment reorientation towards the hard magnetic **c** axis occurs.

Both a non-square modulated and an antiferro-para structures are forbidden for a Kramers ion at $T = 0$; their occurence in these Kondo lattices is due to the singlet N-electron ground state induced by the Kondo coupling, which allows an exchange field modulation to induce a local moment modulation. The spin fluctuations evidenced in the ground magnetic phase of YbAgGe could indicate that frustration is operative in the *kagomé*-like lattice of Yb ions. Such fluctuations seem to be a general feature of magnetically ordered frustrated systems. Finally, the observed complexity of the magnetic structures could arise from the interplay of the Kondo coupling and of the frustration of the AF interactions.

Ames Laboratory is operated for the US Department of Energy by Iowa State University under contract No. W-7405-ENG-82. This work was supported by the Director for Energy Research, Office of Basic Energy Sciences (USA).

References

1. G.R. Stewart, Rev. Mod. Phys. **73**, 797 (2001)
2. A.P. Ramirez, *Handbook of magnetic materials* (Elsevier, 2001), Vol. 13, p. 423
3. D. Kaczorowski, A. Leithe-Jasper, P. Rogl, H. Flandorfer, T. Cichorek, R. Pietri, B. Andraka, Phys. Rev. B **60**, 422 (1999)
4. O. Trovarelli, C. Geibel, R. Cardoso, S. Mederle, R. Borth, B. Buschinger, F. M. Grosche, Y. Grin, G. Sparn, F. Steglich, Phys. Rev. B **61**, (2000) 9467
5. K. Katoh, Y. Mano, K. Nakano, G. Terui, Y. Niide, A. Ochiai, J. Magn. Magn. Mat. **268**, 212 (2004)
6. E. Morosan, S.L. Bud'ko, P.C. Canfield, M.S. Torikachvili, A.H. Lacerda, J. Magn. Magn. Mat. **277**, 298 (2004)
7. K. Umeo, K. Yamane, Y. Muro, K. Katoh, Y. Niide, A. Ochiai, T. Morie, T. Sakakibara, T. Takabatake, J. Phys. Soc. Jpn **73**, 537 (2004)
8. S.L. Bud'ko, E. Morosan, P.C. Canfield, Phys. Rev. B **69**, 014415 (2004)
9. Y. Tokiwa, A. Pikul, P. Gegenwart, F. Steglich, S.L. Bud'ko, P.C. Canfield, Phys. Rev. B **73**, 094435 (2006)
10. P.G. Niklowitz, G. Knebel, J. Flouquet, S.L. Bud'ko, P.C. Canfield, Phys. Rev. B **73**, 125101 (2006)

11. E. Morosan, S.L. Bud'ko, Y.A. Mozharivskyj, P.C. Canfield, Phys. Rev. B **73**, 174432 (2006)
12. E. Morosan, S.L. Bud'ko, P.C. Canfield, Phys. Rev. B **72**, 014425 (2005)
13. T. Matsumura, H. Ishida, T.J. Sato, K. Katoh, Y. Niide, A. Ochiai, J. Phys. Soc. Jpn **73**, 2967 (2004)
14. B. Fåk, D.F. McMorrow, P.G. Niklowitz, S. Raymond, E. Ressouche, J. Flouquet, P.C. Canfield, S.L. Bud'ko, Y. Janssen, M.J. Gutmann, J. Phys.: Condens. Matter **17**, 301 (2005)
15. B. Fåk, Ch. Rüegg, P.G. Niklowitz, D.F. McMorrow, P.C. Canfield, S.L. Bud'ko, Y. Janssen, K. Habicht, Physica B **378–380**, 669 (2006)
16. P.C. Canfield, B. Fåk, private communication
17. M. Rams, K. Królas, K. Tomala, A. Ochiai, T. Suzuki, Hyperfine Interactions **97/98**, 125 (1996)
18. M. Rams, K. Królas, P. Bonville, J.A. Hodges, Z. Hossain, R. Nagarajan, S.K. Dhar, L.C. Gupta, E. Alleno, C. Godart, J. Magn. Magn. Mat. **219**, 15 (2000)
19. A. Abragam, B. Bleaney, *Electron paramagnetic resonance of transition ions* (Clarendon Press, 1969)
20. P. Bonville, J.A. Hodges, P. Imbert, F. Hartmann-Boutron, Phys. Rev. B **18**, 2196 (1978)
21. P. Bonville, B. Malaman, E.Ressouche, J.-P. Sanchez, M. Abd-Elmeguid, C. Geibel, O. Trovarelli, Europhys. Lett. **51**, 427 (2000)
22. E. Bertin, P. Bonville, J.P. Bouchaud, J.A. Hodges, J.P. Sanchez, P. Vulliet, Eur. Phys. J. B **27**, 347 (2002)
23. I. Mirebeau, A. Apetrei, J. Rodríguez-Carvajal, P. Bonville, A. Forget, D. Colson, V. Glazkov, J.P. Sanchez, O. Isnard, E. Suard, Phys. Rev. Lett. **94**, 246402 (2005)
24. J.A. Blanco, D. Gignoux, D. Schmitt, Phys. Rev. B **43**, 13145 (1991); J.A. Blanco, D. Gignoux, D. Schmitt, Phys. Rev. B **45**, 2529 (1992)
25. P. Bonville, E. Bauer, J. Phys.: Condens. Matter **8**, 7797 (1996)
26. J. Rossat-Mignod, J.-M. Effantin, P. Burlet, T. Chattopadhyay, L.-P. Regnault, H. Bartholin, C. Vettier, O. Vogt, D. Ravot, J.-C. Achard, Jour. Magn. Magn. Mat. **52**, 111 (1985)